UNIVERSIDAD NACIONAL DE COLOMBIA
SEDE MEDELLÍN
FACULTAD DE MINAS

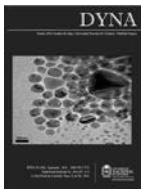

DYNA
http://dyna.medellin.unal.edu.co/

Thermal dielectric and Raman studies on the KNO_3 compound high-temperature region

Fabian Fernando Jurado-Lasso, Natahly Jurado-Lasso, Jaime Alonso Ortiz-Gómez & Jesús Fabian Jurado

Lab. de Propiedades Térmicas Dieléctricas de Compositos, Departamento de Física y Química, Universidad Nacional de Colombia, Sede Manizales, Colombia. fernandoj_27@hotmail.com, natha_sw@hotmail.com, jaortizg@unal.edu.co, jfjurado@unal.edu.co

Received: December 15th, 2015. Received in revised form: July 25th, 2016. Accepted: August 11th, 2016.

Abstract
Calorimetric measurements for a heating-cooling cycle determine the transition temperature and enthalpy of the phases present in the KNO_3compound. The effects correlated within the ionic conduction of the KNO_3 compound were studied by impedance spectroscopy measurements in a frequency range from 0.1 to 10 MHz for a cooling cycle. The imaginary part of the impedance with a frequency between 200 and 100°C showed a displacement of the Debye-like peak in the lower frequency direction. This displacement indicates an increase in the relaxation times of ionic conductivity by jump. In the dielectric formalism module, the imaginary part showed an asymmetric peak as a correlation consequence in the cationic diffusion. Also the registers demonstrated that the process is thermally activated, with activation energy that is very close to the one obtained for dc conduction. From these results, it can be inferred that both, diffusion and conductivity mechanisms have the same origin. The Raman spectroscopy measurements, based on temperature (when cooling), allowed for correlation on each of the adopted phases and for changes in normal active modes of the isolated groups D_{2h} through the evolution of the active modes v_3 and v_2.

Keywords: ionic conduction; impedance spectroscopy, Raman spectroscopy.

Estudios térmicos dieléctricos y Raman del compuesto KNO_3 en la región de alta temperatura

Resumen
Medidas DSC para un ciclo de enfriamiento-calentamiento permiten determinar las temperaturas y entalpías de transición de fases del compuesto KNO_3. Efectos correlacionados en la conducción iónica del compuesto KNO_3, fueron estudiados por medidas de espectroscopia de impedancia en el rango de frecuencia de 0.1 a 10 MHz, para un ciclo de enfriamiento desde 200 a 100°C. La tendencia de la impedancia parte imaginaria con la frecuencia y la temperatura, mostró un desplazamiento del pico "Debye-like" hacia la región de menor frecuencia, este corrimiento indica un aumento en los tiempos de relajación en la conducción iónica por salto. El módulo dieléctrico parte imaginaria, mostró un pico asimétrico como consecuencia de correlaciones en la difusión catiónica, así también, se evidencia que el proceso es térmicamente activado con energía de muy próxima a la obtenida para la conducción dc. Los resultados apuntan a inferir que los dos mecanismos de difusión y conductividad tienen el mismo origen. Medidas de espectroscopia Raman en función de la temperatura (enfriando), permitió correlacionar en cada una de las fases adoptadas los cambios en los modos activos normales de los grupos aislados D_{2h}, a través de la evolución de los modos activos v_3 y v_2.

Palabras claves: conducción iónica; espectroscopia de impedancia; espectroscopia Raman.

1. Introduction

KNO_3 is a compound that strongly depends on temperature and pressure. For this reason enormous efforts have been undertaken in order to establish the dynamics and stability of the phases' diversity that the compound has. For example, in normal conditions, KNO_3 has a non-polar rhombic structure, known as aragonite phase II (α), with a

How to cite: Jurado-Lasso, F.F.; Jurado-Lasso, N.; Ortiz-Gómez, J.A. & Jurado, J.F. Thermal dielectric and Raman studies on the KNO3 compound high-temperature region DYNA 83 (198) pp. 244-249, 2016.

© The author; licensee Universidad Nacional de Colombia.
DYNA 83 (198), pp. 244-249, Septiembre, 2016. Medellín. ISSN 0012-7353 Printed, ISSN 2346-2183 Online
DOI: http://dx.doi.org/10.15446/dyna.v83n198.54693

Pmcn space group [1-6]. In a heating process, at around 130°C, the compound has a rhombohedral formation with a non-polar space group R-3m, called phase I (β). If the compound is stabilized in phase I and then cooled, the material transitions to Phase III at a temperature close to 124 °C, with R-3m symmetry. The most important particularity of this phase is the polarization of the charge along the direction <001> (-axis). This phase is considered slightly metastable. The technological interest of the compound is focused on phase III (ferroelectric), in which there is a possibility of being used as an active element in electro-devices (capacitors and volatile memories, among others) due to its excellent piezoelectric and ferroelectric properties. Great experimental efforts have been made in order to establish the dynamic of the transition order-disorder, which is thermally activated and mainly related to the rotation of NO_3^- group around the *c* axis (trigonal axis) [7,8]. Within the phase transitions of the compound, there have also been some theoretical models applied in the interest of understanding and clarify the physics, [9-11]. Calorimetric measurements are reported for heating-cooling cycles, and they precisely determine the transition temperature and its nature [12-14]. In many cases, a dependence on the thermal history has been detected. By using Raman spectroscopy measurements, we demonstrated the correlation between the origin of the crystal structure and the active Raman modes in the compound for all of the existent phases [10,15-18]. In this work, we report the results obtained for differential scanning calorimetry (DSC), spectroscopy impedance (EI), and Raman spectroscopy as a function of temperature for KNO_3, in order to help establish the existent correlations among the structural organization, vibrational order, and dielectric transportation in the high temperature region.

2. Experimental Set-up

The potassium nitrate powder with a high purity (≥99.9 %) used in this study was supplied by Panreac Química SAU.

The structural order of the compound at room temperature was established by powder X-Ray diffraction by using the A8 Advance Bruker AXS equipment (2θ Bragg –Brentano geometry), which worked at 40 kV and 40 mA. The X-ray diffraction patterns were collected in step-scanning mode with 0.02 steps using a $CuK_{\alpha 1}$ (λ=1.54056 Å) wave. Raman scattering spectra were measured using a Raman apparatus (LabRam HR800 Yvon Horiba) with laser (λ=473 nm). The incent and scattering beams were focused with a microscope that had a x20 objective, which allowed for the sample surface to be probed with a ~20μm-spot- sized laser. The spectral range from 150 to 400 cm^{-1} and temperature range from 20 to 200°C. The heating system was performed by using a micro-furnace built in our laboratory, with a precision of ±1.0ºC. It was heated in situ for each register and was kept in the isotherm for 10 min. The thermal behavior was studied with TA Instruments DSC-Q2000 apparatus. The sample was closed in hermetically-sealed aluminum pans in the range from -90 to 350°C at a heating rate of 10°C/min for both heating and cooling cycles under a nitrogen flow of 50 ml/min.

The impedance measurements were carried out by using a LCR meter Solatron 1260 controlled by a computer over a frequency range from 100 to 10 MHz. There was a potential of 500 mV. The possible nonlinear effects due to the amplitude of the voltage were checked 1.0 V in all of the frequency range for a typical configuration of a two-electrode iron cell with a steel/material/steel configuration. The cell was placed into a sealed temperature-controlled (homemade) chamber. The temperature of the sample was registered by using a K-type thermocouple and then located close to the sample with a precision of ±0.5°C. Each sample was equilibrated at the experimental temperature for at least 10 min before the measurements were made. The impedance of the KNO_3 sample was recorded at various isotherms over a temperature range from 23 to 200°C in air.

3. Results and discussion

3.1. X-Ray diffraction

Fig.1 shows the diffractogram at room temperature for KNO_3. If we consider the initial crystals given by data-base code ICSD -260601 [19] and the Rietveld analysis with Topas software V.4.2 as parameters, the crystallographic parameters could be established as *a*=5.213(59) Å and *c*=8.162(10) Å; this is in agreement with some published data [9,19].

3.2. DSC Calorimetry

Fig. 2 shows the DSC thermogram of KNO_3 for a cooling-heating cycle from -90 to 350°C.

The DSC measurements for an endothermic reaction also show that in the high temperature region, the compound goes from liquid state to phase I(β) at around 332.1°C and enthalpy of 97.3 J/g. This is followed by the transition from phase III(γ) at around 121.7°C and enthalpy of 27.1 J/g. When heating the compound that is departing from the minor temperature area, it presents a transition from the exothermic phase at around 62.4°C with a formation enthalpy of 11.8 J/g in the recovering phase II(α). When the temperature is increased, the system shows a transition from phase I(β) at

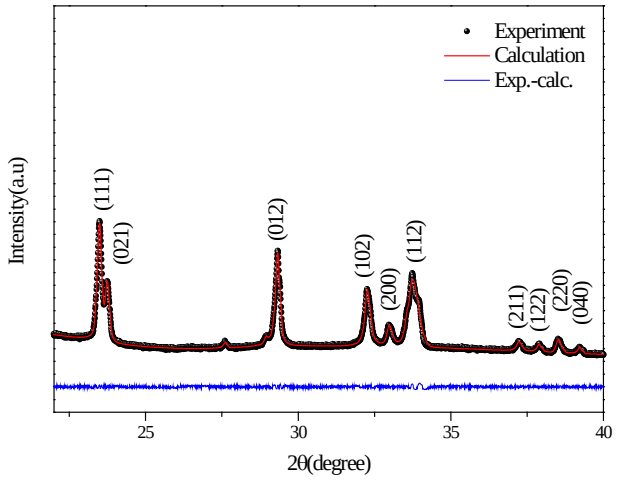

Figure 1. X-Ray powder pattern of KNO_3 at room temperature. The spectral lines were indexed considering the R-3m group.
Source: The authors.

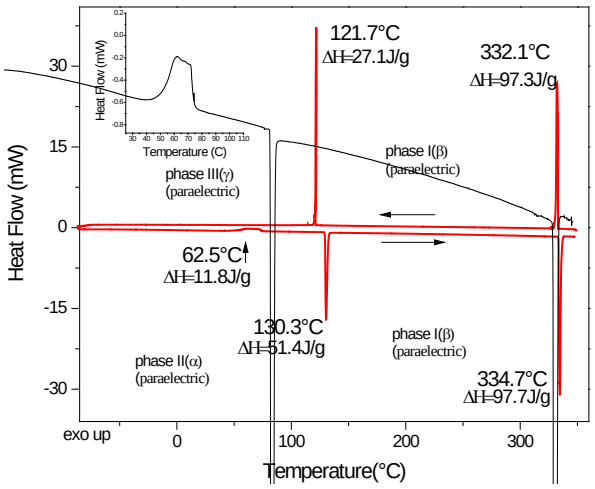

Figure 2. DSC thermogram of KNO_3, for a cooling-heating cycle from -90 to 350°C. The inset shows enlargement of the exothermic transition near 62.5°C. The arrows indicate the direction of the heating-cooling cycle.
Source: The authors.

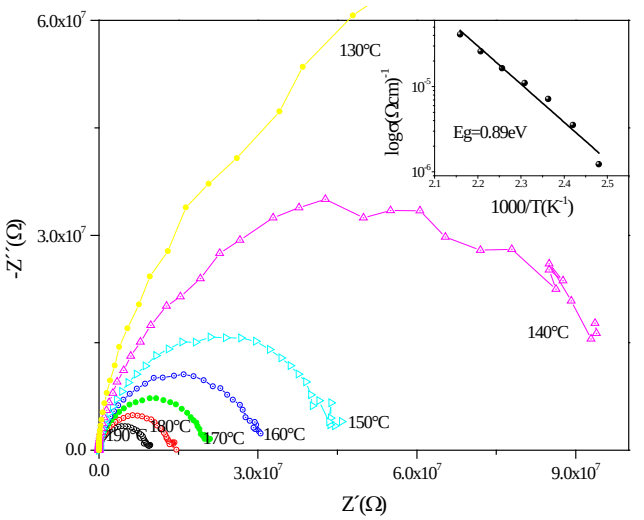

Figure 3. Cole-Cole (Nyquist) plot of KNO_3 impedance measured at different temperatures. The inset shows plots of dc conductivity of Vs 1000/T(K). The line represents the better lineal adjustment.
Source: The authors.

Table 1.
The transformation enthalpies during heating and cooling modes.

Modes (Cooling/Heating)	Transition temperature °C	Phase	Enthalpy J/g
Cooling	332.1	I(β)	97.3
Cooling	121.7 124[28]	III(γ)	27.1
Heating	62.5 110[28]	II(α)	11.8
Heating	130.3 130 [28]	I(α)	51.4
Heating	334.7	I(β)	97.7

Source: The authors.

about 130.3°C and an enthalpy of 51.5 J/g. When the temperature is increased, the system melts at about 334.7°C with a transformation enthalpy of 96.7 J/g. The results obtained in this study agree with those reported in the literature [4,12,28]. The transformation enthalpies during heating and cooling modes are show in Table 1.

Comparing the enthalpy transformation values during phase III(β), phase II(α), and phase I(β) respectively, we can concluded that the three transitions come from a different origin. Phase III's transition is an order-disorder transition, which occurs in a very narrow temperature region.

3.3. Impedance spectroscopy

Typical Nyquist (–Z´´versus Z´) plots of impedance data at different isotherms are shown in Fig. 3 between 190 to 130°C for a KNO_3 sample. The dielectric response is represented by an *RC* circuit that is connected in parallel, which is reduced to a pure resistance for high and low frequencies. For all measurements in every temperature range, the circle we described goes through the origin in the high frequency region. For the low frequency region, the measurement does not show any effects related to the electrode/material interface. The dc conductivity was calculated from the Nyquist plots, as is usual in these cases.

Additionally, the extrapolation arc to the Re*Z* axis (which is in the interception) was the bulk resistance *R* of the KNO_3. The most appropriate ones were selected and the formula $\sigma=d/RA$ was used, where *d* is the thickness and *A* is the contact area of the material and the electrodes.

Fig. 4 shows the imaginary part of impedance variation with the frequency for different temperatures. The movement of the Debye-like peak, which goes in the direction the lower frequency when temperature decreases, supposes an increase in the relaxation times for ionic conductivity by jump. Moreover, the linear dependence of the impedance on the frequency with slope -1, when the temperature is 130°C, shows that conductivity is independent of the frequency for temperatures below this temperature value. The dc conductivity measurements, according to the temperature of the KNO_3 compound, are plotted as: $\ln\sigma$ vs. 1000/T, and they are displayed in the inset of Fig.3. We found an Arrhenius model by using the least square analysis for corresponding data. From the Arrhenius type, we determined the activation energy Eg, calculated using the formula: $\sigma(T)=\sigma_0\exp(-E_g/kT)$, where *k* is the Boltzmann constant, T is the absolute temperature and σ_o the exponential pre-factor. The activation energy calculated in this case was of E_g=0.89 eV, which is close to what the references [20,21] report.

An alternative method in the time domain, to distinguish the correlation effects in the conductivity relaxation, can be obtained from the complex modulus formalism [22,23] $M^*(\omega)=1/\varepsilon^*=j\omega C_0 Z^*(\omega)$, where $j=\sqrt{-1}$, $\omega=2\pi f$ is the angular frequency and C_o is the vacuum capacitance of the cell. The most relevant part of this formalism is that the electrode effects can be suppressed at a low frequency.

Fig. 5 shows a M''/M''_{max} normalized data versus log(*f*) relative to the temperature given. It shows a displacement in the maximum (M''_{max}) towards the minor frequency region when the temperature decreases. In this formalism, the peak marked the transition regime for the ion mobility that is present in the compound: from a long range (dc) to a short

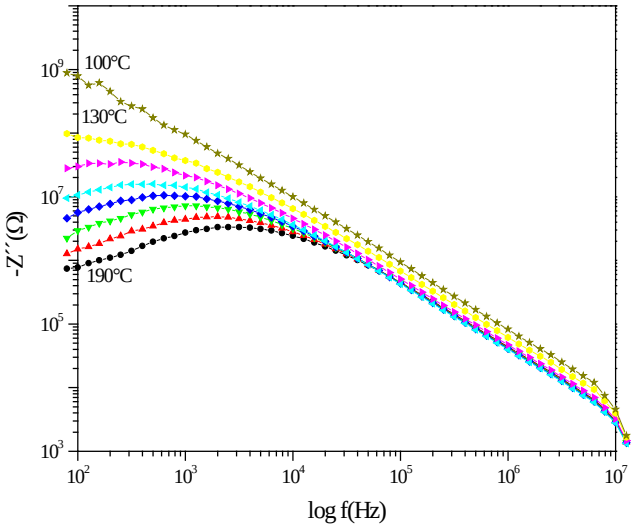

Figure 4. Variation in the imaginary part of impedance with frequency for KNO_3. When the temperature is 100˚C, the dependence of impedance with frequency has slope -1.
Source: The authors.

range. Furthermore, the asymmetry of the width of the peak, moving away from the ideal value (one), is an indicator that the ionic conduction is a distribution of relaxation times. This moves away even further from the Debye ideal model while the temperature decreases. From the maximum M''_{max}, the relaxation time was determined by using the expression $\omega_{max}\tau=2\pi f_{max}RC=1$, where f_{max} is the frequency relative to $M''_{max,}$ which is the peak corresponding to bulk relaxation.

An Arrhenius-type law is shown to be within the temperature range as it is also exposed that the process is thermally activated (inset Fig.5). The activation energy value related to the relaxation process is close to the energy activation value obtained from $\ln\sigma$ vs. 1000/T. The shape and the width of the peak do not change considerably with temperature decreases. This allows it to be affirmed that, in ionic diffusion, the relaxation process has a correlated effect [22]. Additionally, in the conduction by ion jump, we can find that there is an intrinsic mechanism and that relaxation times are affected by the availability of places. This mechanism is common in many ion conductors [24]

From these results, it can be inferred that conduction is not affected by blocking grain boundaries. It can also be affirmed that the conductivity relaxation peak is not a consequence of dipolar relaxation in bulk materials, as normally happens (bulk materials) [24-26]. However, it is very common that in the M''/M''_{max} vs. log(f) formalism there could be one or more peaks. These represent more relaxation processes of which allocation and interpretation are still very controversial [22,23].

3.4. Raman spectroscopy

The structural change in KNO_3 is mostly related to the change in NO^{-}_3 groups f as well as the natural vibration modes. For example, in normal conditions, KNO_3 is in phase II, and NO^{-}_3 contains a symmetry of D_{2h} [6,27]. According to the selection rules for Raman and infrared absorption, which are characterized eleven normal modes that group into: $v_1(A_1)$, $v_3(E')$, $v_4(E'')$ and $2v$. Experiments have shown that they locate around: 1054, 1383, 715 and 1664 cm^{-1}, respectively [6, 27].

Fig. 6 shows the presence of the three phases adopted in KNO_3, due to the change in the compound temperature, for a cooling process from 173 to 22°C. Each phase is characterized by the presence and location of the peaks that are related to the isolated D_{2h} group's natural mode of vibration. During the temperature lowering process the change dynamic of v_3 and $2v$ modes is displayed, respectively. When the temperature reaches approximately 173˚C the material is in phase I. According to the selection rules, it has been determined that, there are 9 existent Raman modes in this phase [10,15– 18], from which it is possible to determine the presence of the ones located in: 719, 1052, 1356, 1420 and 1667 cm^{-1}. In this phase, the most relevant factor of these measurements is the overlapping v_3 mode, which is located approximately in 1356 and 1420˚C, respectively (Fig. 7).

When the temperature of the compound is around 43˚C, the material adopts phase III. The most important factor in these conditions is the splitting of the v_3 mode into four main peaks that are located around: 1351, 1381, 1406 and 1441 cm^{-1}, respectively. Progressive splitting of the vibrational mode occurs while the temperature decreases. This dynamic is considered to be a strong indicator of the nature of the phase change, which gradually assimilates when its temperature lowers. When the temperature is at 24˚C, the material is in phase II (Fig.7).

The most important characteristic of this phase change dynamic is centered on v_3 mode changing, while temperature varies, to finally define at this temperature, a double located around 1347 and 1362 cm^{-1}, respectively. It is also important to note that there is a splitting of the $2v_2$ mode in the peaks located around 1654 and 1687 cm^{-1}, respectively. However, there is a persistence of the peaks close to 1387 and 1441 cm^{-1}, respectively. This indicates the presence of a residual

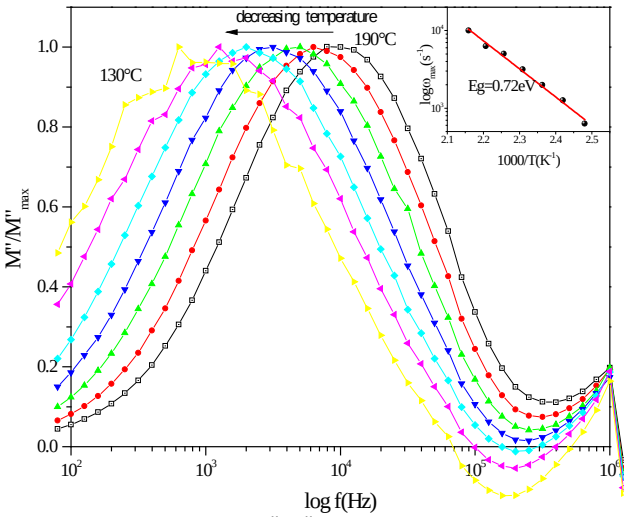

Figure 5. Plots of modulus M''/M''_{max} versus log(f) for KNO_3 at various temperatures. The inset shows an Arrhenius plot of $\log\omega_{max,}$ which is plotted against 1000/T. The line represents the better lineal adjust.
Source: The authors.

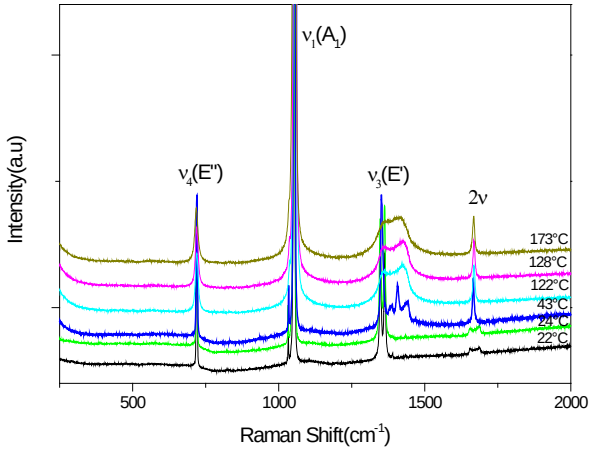

Figure 6. The evolution of the spectra profiles for the $\nu_4(E'')$, $\nu_1(A_1)$, $\nu_3(E')$, and 2ν of NO^-_3 vibration between 173°C to 22°C during phase I, II, and III transitions.
Source: The authors.

phase III and concurs with the affirmation of the coexistence of phases. From the three phases presented in Fig. 7 it can be inferred that phase III has a better definition of the main basic vibration modes. This could coincide with the concept that states this kind of structural order is now a charge order (as in the case of the ferroelectric phase).

4. Conclusions

The calorimetric measurements allowed us to determine the phase transition temperatures and compare the respective enthalpy values of the transitions. This comparison allows us to distinguish the transition order-disorder, which is characterized by its very narrow transformation enthalpy value. KNO_3 in the high temperature region showed that dc ionic conductivity is thermally activated by the Arrhenius-type. The impedance (imaginary part) revealed that the dc ionic conduction is caused by the charge carriers jumping. With

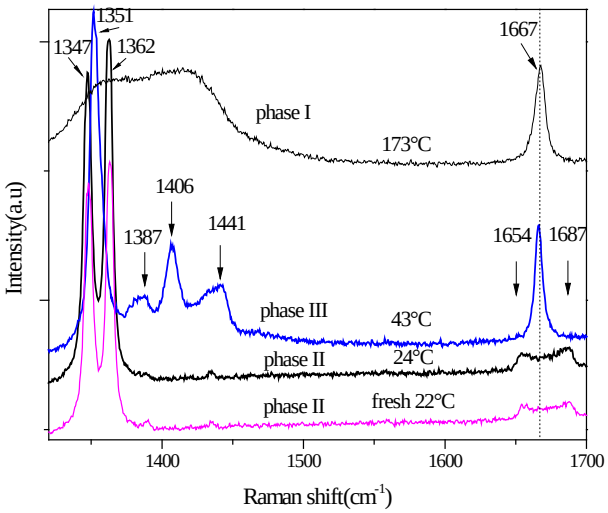

Figure 7. Comparison of Raman data between KNO_3 phases I, II and III for a cooling cycle. The arrow marked their symmetry labels under are phase mode.
Source: The authors.

the temperature increase, the distribution of the relaxation times displaces towards the lower frequency region. Dielectric formalism modulus showed how the relaxation processes were modified, causing a change of structural order and a short-range temperature effect. Additionally, this was an Arrhenius type process and thermally activated the process. The respective activation energies' values lead us to the conclusion that they have the same dc conductivity origin, as well as the ion jump probability, among available sites.

The Raman spectroscopy allowed us to establish the change of phases dynamic as well as determine that phase III presents the best definition of the basic vibrational modes. These results concur with structural organization and charge organization (as in the ferroelectric phase case).

Acknowledgements.

This work was carried out with support from the Research system DIMA at the Universidad Nacional de Colombia.

References

[1] Megahid, N.M., Field dependence of electrical conductivity of powder compacts of (KNO3)1-xCux mixtures, Egyto J.Sol., [Online]. 25, pp. 125-136, 2002. Available at: http://egmrs.powweb.com/EJS/PDF/vo251/125.pdf.

[2] Bartholomew, R.F., A study of the equilibrium KNO3--KNO2(l)+1/202(g) over the temperature range 550-750°C, J.Phys. Chem., [Online]. 72(1), pp. 3442-3446, 1966. Available at: http://pubs.acs.org/toc/jpchax/70/11

[3] Dabra, N., Hundalw, J.S., Sekhar, K.C., Nautiyal, A. and Nath, R., Ferroelectric phase stability studies in spray deposited KNO3: PVA composite films, J. Am. Ceram. Soc., 92(4), pp.834-838, 2009. DOI: 10.1111/jace.2009.92.issue-4/issuetoc

[4] Aquino-Olivos, M.A., Jean-Pierre, E. Grolier, S.L. Randzio, A., Aguirre-Gutiérrez, J. and Garcia-Sanchez, F., Transitiometric determination of the phase diagram of KNO3 between (350 and 650) K and at pressures up to 100 MPa, J. Chem. Eng. [Online]. 55, pp.5497-5503, 2010. Available at: http://pubs.acs.org/toc/jceaax/55/12

[5] Baryshnikov, S.V., Charnaya, E.V., Yu, A., Milinskii, E., Stukova, V., Cheng, T. and Michel, D., Dielectric properties of crystalline binary KNO3–AgNO3 mixtures embedded in nanoporous silicate matrices, Physics of the Solid State, 52(2), pp. 392-396, 2010.

[6] Xu, K., Application of Raman in phase equilibrium studies: The structures of substitutional solid solutions of KNO3 by RbNO3, J. Mat. Science, 34, pp. 3447-453, 1999.

[7] Kumar, N. and Natha, R., Ferroelectric properties of potassium nitrate-polymer composite films, J. Pure Appl. & Ind. Phys. [Online]. 1(1), pp. 21-35, 2010. Available at: http://physics-journal.org/archive-1-1.html

[8] Erdinc, B. and Akkus, H., Ab-initio study of the electronic structure and optical properties of KNO3 in the ferroelectric phase, Phys. Scr. [Online]. 79, pp. 025601-025006, 2009. Available at: http://iopscience.iop.org/issue/1402-4896/79/2

[9] Lu, H.M. and Hardy, J.R., Principles study of phase transitions in KNO3, Phys. Rev. B, [Online]. 44, pp. 7215-7224, 1991. Available at: http://journals.aps.org/prb/issues/44/14

[10] Liu, D., Ullman Behlen, F.G. and Hardy, J.R., Raman scattering and lattice-dynamical calculations of crystalline KNO3, Phys. Rev. B., [Online]. 45(5), pp. 2142-2147, 1992. Available at: http://journals.aps.org/prb/issues/45/5

[11] Porto, M., Maass, P., Meyer, M., Bunde, A. and Dieterich, W., Hopping transport in the presence of site-energy disorder: Temperature and concentration scaling of conductivity spectra, Phy. Rev.B., [Online]. 61(9), pp. 6057-062, 2000. Available at: http://journals.aps.org/prb/issues/61/9

[12] Abdulagatova, I.M., Dvoryanchikov, V.I. and Kamalov, A.N., Measurements of the heat capacities at constant volume of H2O and (H2O + KNO3), J. Chem. Thermodynamics, [Online]. 29, pp. 1387-1407, 1997. Available at: http://www.sciencedirect.com/science/journal/00219614/29/12

[13] El-Kabbany, F., Abdel-Kader, M.M., Tosson, M. and El-Khwass, E., Kinetics of the ferroelectricalbehaviour of a thin layer of phase III KNO3, Thermochimica Acta, [Online]. 256, pp. 281-289, 1995. Available at: http://www.sciencedirect.com/science/journal/00406031/256/2
[14] Font, J. and Muntasell, J., Thermobarometric study of KNO3 phase transitions, Thermochimica Acta, [Online]. 293, pp. 167-170, 1997. Available at: http://www.sciencedirect.com/science/journal/00406031/293/1-2
[15] Balbaski, M., Teng, M.K. and Nusimovici, M., Raman scattering in KNO3 phases I, II, and III, Phy. Rev. [Online]. 176(3), pp. 1098-1106, 1968. Available at: https://journals.aps.org/pr/issues/176/3
[16] Scott, J.F. and Zhang, M.-S., Raman spectroscopy of submicron KNO3 films, Phys. Rev.B, [Online]. 35, pp. 4044-4051, 1987. Available at: http://journals.aps.org/prb/issues/35/8
[17] Murugan, R., Huang, P.J., Ghule, A. and Chang, H., Studies on thermal hysteresis of KNO3 by thermo-Raman spectroscopy, Thermochimica Acta, [Online]. 346, pp. 83-90, 2000. Available at: http://www.sciencedirect.com/science/journal/00406031/346/1-2
[18] Loudon, R., The Raman effect in crystal, Advan. Phys., 13, pp. 423-482, 1964. Available at: http://www.tandfonline.com/toc/tadp20/13/52?nav=tocList
[19] Freney, E.J., Garvie, L.A.J., Groy, T.L. and Buseck, P.R., Growth and single-crystal refinement of phase –III potassium nitrate, KNO3, Acta Cryst., [Online]. B65, pp. 659-663, 2009. Available at: http://scripts.iucr.org/cgi-bin/paper?S0108768109041019
[20] Singh, A. and Smith, A.M., Dielectric and electrical conductivity studies in potassium nitrite. J. phys. D: Appl. Phys. [Online]. 4, pp. 560-566, 1971. Available at: http://iopscience.iop.org/issue/0022-3727/4/4
[21] Mansingh, A. and Smith, A.M., Dielectric dispersion in the paraelectric phase of potassium nitrate, J. Phys. D: Appl. Phys., [Online]. 4, pp. 1792-1796, 1971. Available at: http://iopscience.iop.org/issue/0022-3727/4/11
[22] Elliott, S.R., Use of the modulus formalism in the analysis of ac conductivity data for ionic glasses, Journal of Non-Crystalline Solids, [Online]. 170, pp. 97-100, 1994. Available at: http://www.sciencedirect.com/science/journal/00223093/170/1
[23] Svare, I., Borsa, F., Torgeson, D.R., Martin, S.W. and Patel, H. Use of the modulus formalism in the analysis of ac conductivity data for fast ion conductors, Journal of Non-Crystalline Solids, [Online]. 185, pp. 297-300, 1995. Available at: http://www.sciencedirect.com/science/journal/00223093/185/3
[24] Jurado, J.F., Trujillo, J.A., Mellander, B-E. and Vargas, R.A., Correlated ion diffusion in gamma-Ag0.7Cu0.3I, S. State. Ionic, [Online]. 176, pp. 985-990, 2005. Available at: http://www.sciencedirect.com/science/journal/01672738/176/9-10
[25] Mellander, B.-E. and Albinsson, I., in Solid State Ionics: New Developments edited. Chowdari, B.V.R et al., World Scientific, Singapore, [Online]. 1996, pp. 83-87. Jurado, J.F., Játiva, J.A., Metal-insulator transition and hopping conduction mechanisms in the La0.7Ba0.3MnO3 compound, J. Mag. Magn. Mate., 335, pp. 6-10, 2013. Available at: http://www.sciencedirect.com/science/journal/03048853/335
[26] Nakamoto, K., Infrared and Raman spectra of Inorganic and Coordination Compounds, 4th ed., Wiley, New York, 1986, pp. 6-20.
[27] Kumar, E. and Natha, R., Ferroelectric properties of potassium nitrate-polymer composite films, J. Pure Appl. & Ind. Phys., [Online]. 1, pp. 21-35, 2010. Available at: http://physics-journal.org/archive-1-1.html

F.F. Jurado-Lasso, received a First Class MSc. degree in Telecommunications Engineering after attending The University of Melbourne, Australia in 2015. Also, he obtained a bachelor degree in Electronics Engineering after studying in The Universidad del Valle, Colombia in 2012. He has also worked with projects related to new materials with an emphasis in Telecommunications.
ORCID: orcid.org/0000-0002-5005-781X.

N. Jurado-Lasso, Bacteriologist for The Universidad del Valle, Colombia. She has also worked with projects related to new materials.
ORCID: orcid.org/0000-0001-6091-4160.

J.A. Oriz-Gomez, is Engineer -Physicist of the Universidad Nacional de Colombia. He has also worked with projects related to new materials.
ORCID: orcid.or/000-0001-8972-1805

F.J. Jurado, is Dr. Ciencias Física (titular professor) worked on Condensed Matter, total experience –20 years with about fifteen original article research publications in international journal as a co-author. He is the leader of Laboratorio de Propiedades Térmicas Dieléctricas de Compositos, Universidad Nacional de Colombia Sede Manizales.
ORCID:orcid.org/0000-0001-5193-8566.

UNIVERSIDAD NACIONAL DE COLOMBIA
SEDE MEDELLÍN
FACULTAD DE MINAS

Área Curricular de Ingeniería
Geológica e Ingeniería de Minas y Metalurgia

Oferta de Posgrados

Especialización en Materiales y Procesos
Maestría en Ingeniería - Materiales y Procesos
Maestría en Ingeniería - Recursos Minerales
Doctorado en Ingeniería - Ciencia y Tecnología de Materiales

Mayor información:

E-mail: acgeomin_med@unal.edu.co
Teléfono: (57-4) 425 53 68